PHILOSOPHICAL TRANSACTIONS OF THE ROYAL SOCIETY A MATHEMATICAL, PHYSICAL & ENGINEERING SCIENCES

Ordered Bicontinuous Films of Amphiphiles and Biological Membranes

J. Charvolin and J.-F. Sadoc

Phil. Trans. R. Soc. Lond. A 1996 **354**, 2173-2192
doi: 10.1098/rsta.1996.0097

Ordered bicontinuous films of amphiphiles and biological membranes

By J. Charvolin and J.-F. Sadoc

[1] *CNRS, 3 rue Michel-Ange, 75794 Paris cedex 016, France*
[2] *Laboratoire de Physique des Solides, Bâtiment 510, Université de Paris Sud, 91405 Orsay, France*

Films of amphiphilic molecules form layers, with complex as well as simple topologies. Well-defined examples of surfaces in chemical systems with the topologies of the subtly related P, D and G triply periodic minimal surfaces (TPMS) are examined. The analysis is extended to the biological structures of etioplasts found in green plants which are more complex. The analysis shows how local order constrains global order. Local order may indicate a metric only achievable in a higher dimensional space and the requirements of our actual space lead to ingenious compromises.

1. Introduction

In the presence of water the hydrophobic paraffinic tails and the hydrophilic polar heads of amphiphilic molecules segregate to form films as shown in figure 1. These films are not necessarily planar but can have much more complicated topologies (see, for example, Nelson *et al.* 1989; Dubois-Violette & Pansu 1990; Lipowsky 1992; Gelbart *et al.* 1994) varying with temperature and water content.

We will consider only ordered bicontinuous structures and we will be particularly concerned with triply periodic minimal surfaces (TPMS) which separate space into two infinite subspaces without self-intersection. Structures related to TPMS may form spontaneously in physico-chemical systems (particularly liquid crystals) and in biological systems (membranes within cells).

The shape of a film embedded in R^3 is defined by the values at every point of the two principal curvatures C_1 and C_2 of its mean surface. Its energy can then be written as

$$E_c = \tfrac{1}{2}\kappa(C_1 + C_2 - C_0)^2 + \bar{\kappa}C_1C_2,$$

where κ and $\bar{\kappa}$ are the elastic constants of mean and Gaussian curvatures of the film, respectively, and C_0 is its spontaneous curvature (Helfrich 1990). A symmetric film has $C_0 = 0$ and possible shapes with minimal energy for a given topology are such that the mean curvature $C_1 + C_2$ is zero (as the second term in energy depends only on the topology). This is the mathematical definition of a minimal surface. Either $C_1 = C_2 = 0$, when the surface is planar with zero Gaussian curvature, or $C_1 = -C_2$, when the surface is a hyperbolic surface with negative Gaussian curvature. A limited element of the latter is saddle-shaped, as shown in figure 2, but there exists no surface with constant negative Gaussian curvature in our three-dimensional space R^3. However, curved patches or finite elements with negative Gaussian curvature can be joined smoothly together in R^3 in a great variety of ways (Schoen 1970).

Phil. Trans. R. Soc. Lond. A (1996) **354**, 2173–2192
Printed in Great Britain

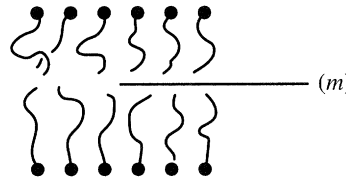

Figure 1. A patch of a film made of two facing interfaces of amphiphilic molecules and its mid-surface (m). The patch is symmetric with respect to this mid-surface.

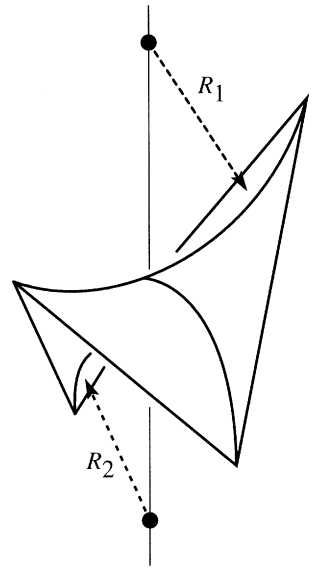

Figure 2. An element of saddle is minimal if $R_1 = -R_2 = R$, its area goes as R^2 and that of a surface parallel to it at a distance d on either side goes as $R^2 - d^2$.

The structures of films of amphiphilic molecules in liquid crystals and some biological membranes (Mariani *et al.* 1988; Lindblom & Rilfors 1989; Seddon 1989; Thomas *et al.* 1986) correspond to some of these solutions. In all cases except those related to the I-WP surface (Hyde 1990), the surface separates space into two congruent or oppositely congruent subspaces. In some biological cases the membrane separates two different subspaces and their organization shows five-fold local symmetries unknown in the liquid crystalline cases (Gunning & Steer 1975). Here liquid crystal and biological cases will be considered together.

2. Liquid crystals of amphiphiles

In amphiphile–water phase diagrams close to the lamellar phase domain (Mariani *et al.* 1988; Lindblom & Rilfors 1989; Seddon 1989; Thomas *et al.* 1986) where the concentration of amphiphile is high, cubic phases are observed, the structures of which are related to the TPMS.

(*a*) *Bicontinuous cubic structures and the three basic TPMS*

Three structures, D, P and G, with space groups $Pn\bar{3}m$, $Im\bar{3}m$ and $Ia\bar{3}d$, are found which correspond to the three basic TPMS built by joining minimal saddles smoothly so that the whole infinite surface is minimal everywhere and triply periodic. If there

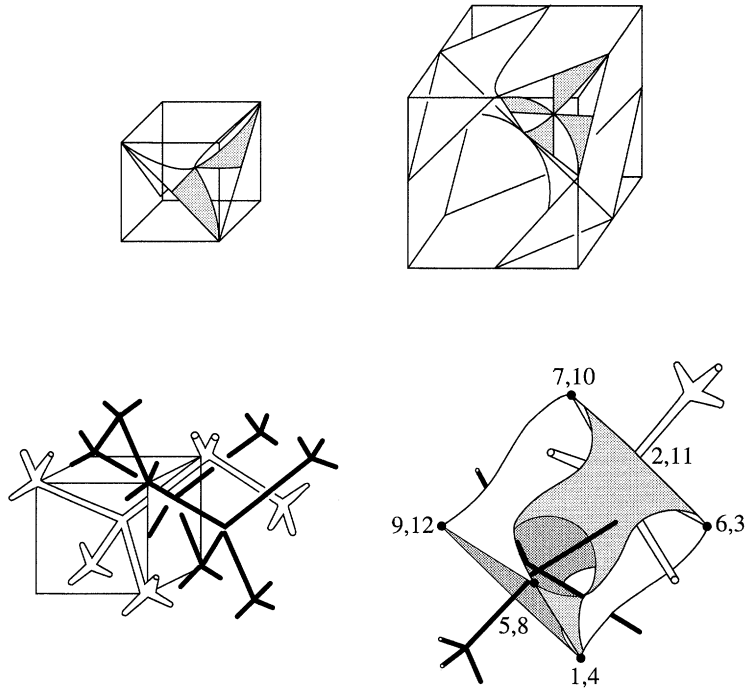

Figure 3. Schwarz's D (or F) surface: the quadrilateral saddle with eight orthoscheme triangles, the first step of the construction of the surface by assembling six saddles, the two labyrinths of coordination 4 separated by the surface and an elementary cell in which the surface appears as a dodecagonal sheet having vertices assembled in six groups of two.

are straight lines in the surface these must be diad axis symmetries of the periodic structure (Schöenflies 1882; Schwartz 1890). The theory was recently extended to polygonal saddles with curved edges and non-cubic symmetries (Schoen 1970). We consider them in turn.

(*b*) *Schwarz's D surface*

For the D surface the contour of the saddle is a quadrilateral with straight edges which are four of the diagonals of the faces of a cube, as shown in figure 3. These face diagonals become diad axes and repeat the saddle infinitely to give the D surface. Part of the unit cell with space group $Pn\bar{3}m$ and the two congruent labyrinths of connectivity 4 separated by the surface are also shown in figure 3. The saddle drawn in the figure is made up of eight asymmetric triangular units or orthoschemes (Mackay 1985). The orthoscheme triangle has vertex angles of $\frac{1}{2}\pi$, $\frac{1}{4}\pi$ and $\frac{1}{6}\pi$, the sum of which is less than π. The triangle is therefore not Euclidean, and corresponds to a triangle drawn on a hyperbolic surface.

The complete elementary cell, also shown in figure 3, encloses a piece of surface which is an irregular dodecagon of 96 orthoschemes, with short and long edges, the vertices of which are joined in six groups of two. Note that the assembly of 12 orthoscheme triangles by their $\frac{1}{6}\pi$ vertices is a hexagon and that, on the surface, the hexagons are assembled 4×4 around each of their vertices. This $\{6,4\}$ tiling is typical of a hyperbolic surface with negative Gaussian curvature, the tiling of a flat surface with hexagons being $\{6,3\}$. (The Schläfli notation $\{p,q\}$ for a two-dimensional tiling means that the tiling is made of regular polygons having p edges that meet q by q

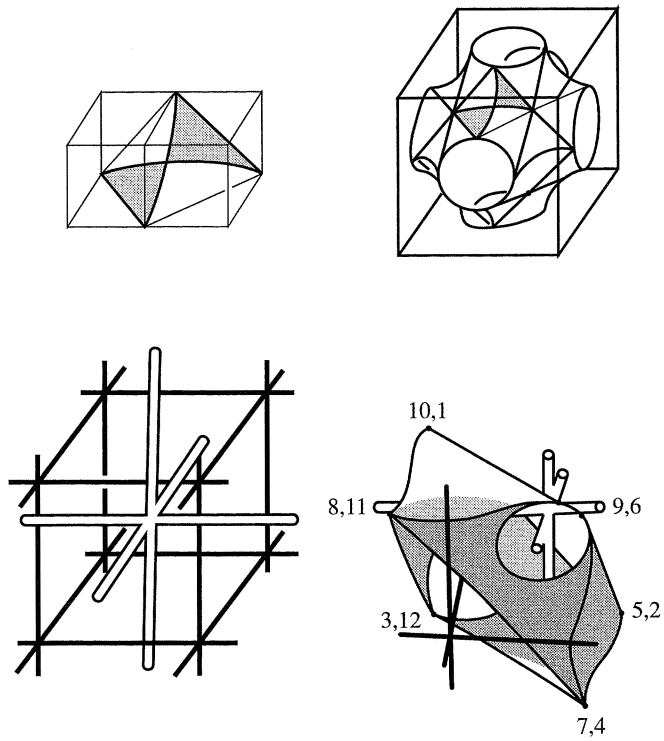

Figure 4. Schwarz's P surface: the quadrilateral saddle with four orthoscheme triangles, an assembly of complete and incomplete saddles building an elementary cell, the two labyrinths of coordination 6 separated by the surface and another elementary cell in which the surface appears as a dodecagonal sheet having vertices assembled in six groups of two (but in a manner different from that of the D surface in figure 3).

at every vertex; notation $\{p, q, r\}$ for a three-dimensional packing means that the packing is made of regular polyhedra, each polyhedron has q p-faces around one vertex and there are r polyhedra around each edge.)

(*c*) *Schwarz's P surface*

The contour of the saddle is a quadrilateral with straight edges which are diagonals of faces of two cubes sharing one common face, as shown in figure 4. The repetition of such a saddle by symmetry along its border leads to the building of the P surface. The unit cell with the space group $Im\bar{3}m$ and the two congruent labyrinths of connectivity 6 separated by the surface are also shown in figure 4.

The saddle drawn in figure 4 is tiled with four orthoscheme triangles having the same vertex angles, $\frac{1}{2}\pi$, $\frac{1}{4}\pi$ and $\frac{1}{6}\pi$, as those of the orthoscheme triangle of the D surface and, therefore, the whole surface also admits a $\{6, 4\}$ hexagonal tiling.

However, although the angles are the same, the triangles are different in the sense that they do not have the same straight and curved edges.

The unit cell can be chosen (following the International Tables for Crystallography) in two ways (figure 4).

As for the D surface, this cell encloses a piece of surface which is an irregular dodecagon of 96 orthoschemes, with short and long edges, the vertices of which are joined in six groups of two but in a manner different to that of the D surface.

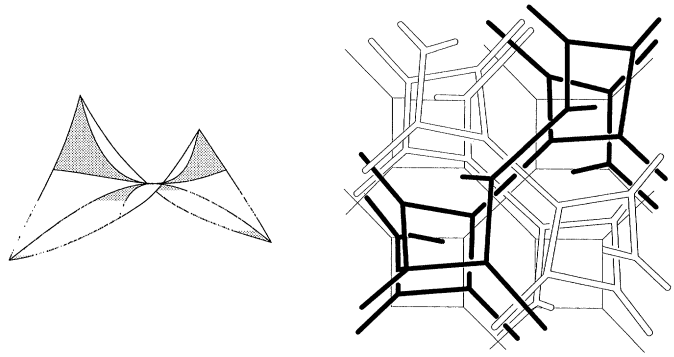

Figure 5. Schoen's G surface: the quadrilateral saddle with curved edges and the two labyrinths of coordination 3 separated by the surface.

(*d*) *Schoen's G surface*

The boundary of the saddle is now a quadrilateral with curved edges, as shown in figure 5. The repetition of such a saddle by symmetry along its border leads to the building of the G surface which has no straight lines in it. Figure 5 shows the two labyrinths of connectivity 3 separated by the surface. Photographs of plastic models can be found in Schoen (1970) and Hyde & Andersson (1984). In this case the two labyrinths are not congruent but oppositely congruent, i.e. they have opposite chiralities. This organization has the space group $Ia\bar{3}d$. The orthoscheme triangle of the surface has vertex angles of $\frac{1}{2}\pi$, $\frac{1}{4}\pi$ and $\frac{1}{6}\pi$, like those of the D and P surfaces, but its three edges are now curved (Schoen 1970). Here also the elementary cell encloses a piece of surface which is an irregular dodecagon of 96 orthoschemes, with short and long edges, but with six vertices joined 3×3 in two groups, the six others being left alone. As for the two other surfaces, the G surface admits a $\{6, 4\}$ hexagonal tiling.

This complicated structure of labyrinths was indeed proposed for a system of amphiphiles more than 20 years ago, from the analysis of X-ray scattering data, at a time when physicists and physical chemists were not concerned with TPMS (Luzzati & Spegt 1967). It has been since identified many times in various systems.

3. Arguments for the existence of such structures in liquid crystals

Arguments can be developed considering the internal mechanics of a film (Charvolin & Sadoc 1994).

The forces acting in amphiphile–water systems need not be detailed at this stage, the important point is that they have components normal to the interfaces which maintain them at a constant distance, and components parallel to the interfaces, the values of which in the aqueous and paraffinic media control the interfacial curvature through a gradient of area along the normal to the interface, as for a bimetallic switch. The structures must therefore reconcile constant interfacial distances and curvatures or constant interfacial distances and symmetric area gradients along the normal to the film.

(*a*) *Frustration*

When thermodynamic conditions are such that the interfaces are flat, the configuration is a periodic stacking of the lamellar phase. When the conditions are otherwise, the interfaces become curved and this is not compatible with a constant distance be-

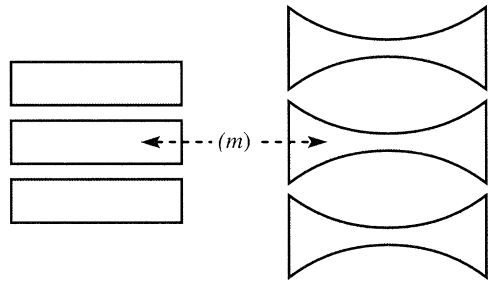

Figure 6. Constant distances between interfaces and zero interfacial curvature are compatible but constant distances between interfaces and non-zero interfacial curvature are not.

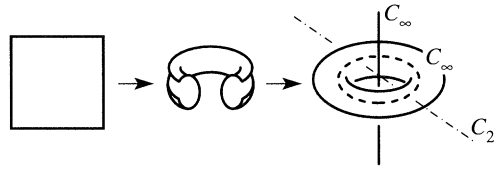

Figure 7. The spherical torus can be built by identification of the opposite sides of a square sheet in S^3 (and therefore admits a $\{4,4\}$ tiling); as this identification is done in a curved space the sheet suffers no distortion, the torus represented here is a stereographic projection in R^3 of the spherical torus in S^3, it admits C_2 and C_∞ symmetry axes.

tween them, as shown in figure 6. We may say, from figure 2, that minimal saddles might be elements of a solution as they allow a symmetric area gradient along their normals. A topological approach demonstrates that the solutions are indeed the assemblies of saddles of the TPMS described above. The conflict between normal and parallel forces is a typical case of frustration. This frustration cannot be resolved in our Euclidean space R^3 but it can be in the curved space S^3, the hypersphere. Thus, ideal structures in S^3 are the starting points in the search for possible optimal structures in R^3. As a curved space is characterized by an angular defect with respect to a flat space, the possible configurations in R^3 differ from the ideal configuration in S^3 by the presence of defects of rotation, or disclinations.

This 'curved-space approach' has led productively to the description of all basic organizations of liquid crystalline structures and of their sequence in phase diagrams (Charvolin & Sadoc 1994). Here we introduce the particular process leading to bicontinuous structures (Charvolin & Sadoc 1987).

(*b*) *Relaxation of the frustration in* S^3

The whole periodic system of frustrated fluid film can be represented without frustration in S^3 by transferring the midsurface of the film onto the surface of the spherical torus T^2 which separates S^3 into two identical subspaces. As this torus has a maximal area in S^3, the interfaces of the film, which are on surfaces parallel to it, have a smaller area than the midsurface, a condition needed to relax the frustration. Also, this torus can be built by identifications of the opposite sides of a square sheet in S^3, as shown in figure 7, and therefore admits a $\{4,4\}$ regular square tiling and C_2 symmetry axes normal to it.

(*c*) *From* S^3 *to* R^3

The nature of the disclinations which intervene in the mapping process is imposed by the C_2 symmetry of the relaxed structure in S^3: they must be $-\pi$ disclinations

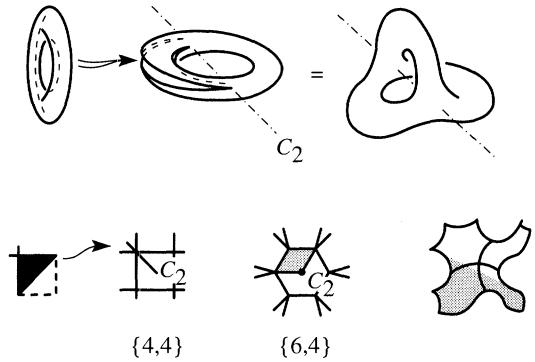

Figure 8. A $-\pi$ disclination around a C_2-axis of the spherical torus transform it into a C_3-axis, the square of the $\{4,4\}$ tiling of the torus is transformed into a hexagon of the $\{6,4\}$ tiling.

normal to the surface (Friedel 1984). Such disclinations preserve the toroidal nature of the surface in S^3, its $\{4,4\}$ square tiling is transformed into a $\{6,4\}$ hexagonal tiling and the C_2 axes become C_3 axes, as shown in figure 8. Thus the surfaces possible in R^3 have a bicontinuous topology and are hyperbolic with $\{6,4\}$ tilings, which are the characteristics of the D, P and G surfaces. Moreover, the space groups $Pn\bar{3}m$, $Im\bar{3}m$ and $Ia\bar{3}d$ are those corresponding to the possible arrangements of C_3 axes in cubic lattices. In the next paragraph we confirm this by showing that there are only three ways to build hyperbolic surfaces of genus three which admit a $\{6,4\}$ tiling in R^3.

4. Relationships between the P, D and G TPMS

The three TPMS, D, P and G, have different symmetries, but have orthoscheme triangles with the same vertex angles of $\frac{1}{2}\pi$, $\frac{1}{4}\pi$ and $\frac{1}{6}\pi$. This suggests topological relationships.

(*a*) *Topological genus*

The topological genus of a surface is the number of its 'handles', e.g. the genus of a simple torus with one hole is 1, whereas that of a sphere is 0. In the case of TPMS which, as such, have an infinite number of handles, the genus may be referred to the primitive unit cell with periodic boundary conditions, as shown in figure 9. If this is done in each of the three cases, for simplicity identifying the extremities of the rods of one labyrinth rather than those of the whole surface, topological graphs of the elementary cells of the three surfaces can be built, as shown in figure 9. These three graphs, although different in their connectivities which are those of the labyrinths, are identical in the sense that they each represent tori with three handles. They each have the topological genus $g = 3$. This gives important information about the Gaussian curvature and about the shape of the piece of surface contained in the elementary primitive cell.

(*b*) *Gaussian curvature*

The integral of the Gaussian curvature $\int C_1C_2$ on a surface is directly related to its topological genus g by the Gauss–Bonnet formula (Hilbert & Cohn-Vossen 1983):

$$\int C_1C_2 \,\mathrm{d}s = 4\pi(1-g).$$

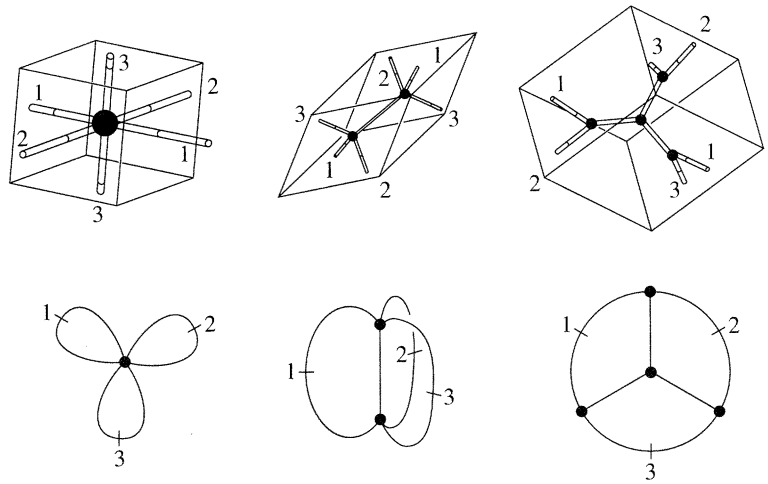

Figure 9. The elementary primitive cells of the simple, face centered and body centered cubic structure of the P, D and G surfaces shown with only one labyrinth. The three topological graphs are obtained by identification of the opposite faces (labelled by 1, 2 and 3) of those elementary cells; in the three case, three loops are formed leading to the genus 3 of the three surfaces.

Thus the value of this integral is 4π for a sphere, 0 for a torus with one hole, values which are well-known from classical geometry, and -8π for a torus with three holes. In our case, as the elementary cells of the three TPMS considered here are equivalent to tori with genus 3, the pieces of surface they contain have the same integrated Gaussian curvature of -8π.

(*c*) *Polygonal cell*

If now we open a torus with genus 3 by cutting its surface, as shown in figure 10, a sheet with twelve edges, i.e. a dodecagon, is obtained. This process is indeed quite general and is related to another topological law stating that a torus with genus g is built by identifications of the edges of a polygon with $4g$ edges two by two (Hilbert & Cohn-Vossen 1983). For instance, a simple torus with one hole is obtained with a 4-gon, i.e. a square as shown already in figure 7, and a torus with genus 3 is obtained with a dodecagon, following a process opposite to that shown in figure 10. Thus, in the cases of the three surfaces studied here, the pieces of surface contained in their elementary cells must have a dodecagonal shape. A topological process for building our three TPMS might therefore be the following: first, the edges of a dodecagon are identified in order to build tori with genus 3, then the handles of the tori are cut, in order to build the elementary cells and, finally, the six branches of each cell connected to branches of similar cells in order to build the periodic structure.

(*d*) *Crystallography in the hyperbolic plane*

The D, P and G surfaces have the same topological genus 3, their orthoscheme triangles have the same vertex angles $\frac{1}{2}\pi$, $\frac{1}{4}\pi$ and $\frac{1}{6}\pi$, the integrals of the Gaussian curvature in their elementary cells have the same value -8π, and the pieces of surface in their elementary cells must be dodecagonal. Moreover, if surfaces D and P are considered, the edges of the orthoscheme triangles, which are directions of principal curvatures in one case, become asymptotic directions in the other, and vice-versa. Thus the three surfaces, although of different symmetries, have many common topological properties. The first may be indeed understood from the second. This can be

PHILOSOPHICAL TRANSACTIONS OF THE ROYAL SOCIETY A MATHEMATICAL, PHYSICAL & ENGINEERING SCIENCES

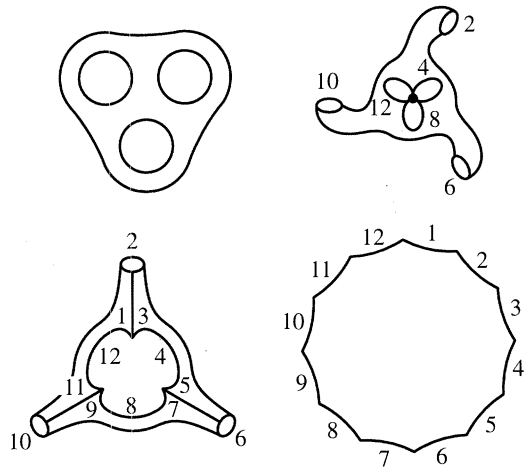

Figure 10. Dissection of a torus of genus 3 into a dodecagonal sheet. If the figure is read the other way round it represent the construction of the torus by identification of the edges of a dodecagon.

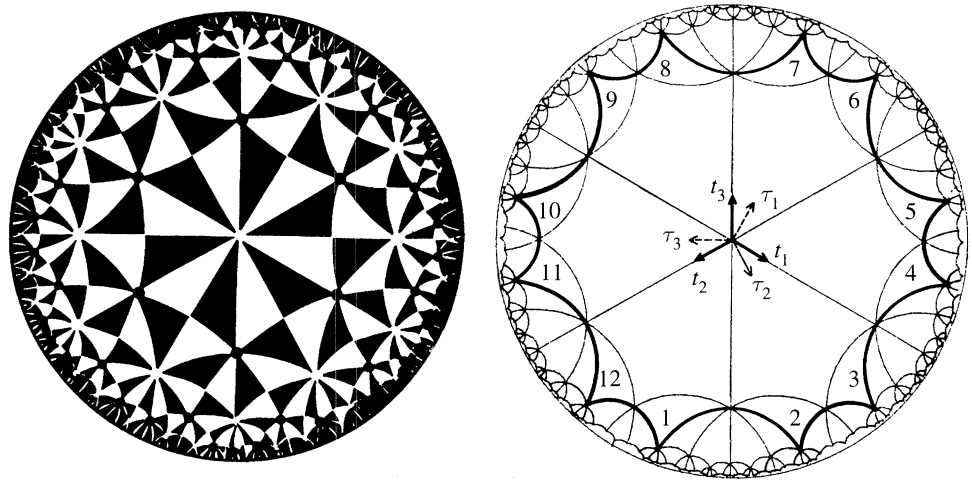

Figure 11. Poincaré's representation of the hyperbolic plane tiled with an orthoscheme triangle with vertex angles of $\frac{1}{2}\pi$, $\frac{1}{4}$ and $\frac{1}{6}\pi$ and its dodecagonal translation cell.

done by examining the properties of the surface having the same Gaussian curvature as the three TPMS, but distributed over the whole surface uniformly—this is called a hyperbolic plane. It does not exist in our three-dimensional Euclidean space, but is embedded in a seven-dimensional space. Fortunately a representation of this surface in a two-dimensional Euclidean plane has been developed by Poincaré (Hilbert & Cohn-Vossen 1983; Coxeter 1961; Sadoc & Charvolin 1989).

(*e*) *The Poincaré representation*

The hyperbolic plane related to our problem is built with the orthoscheme triangle of constant Gaussian curvature with the same vertex angles $\frac{1}{2}\pi$, $\frac{1}{4}\pi$ and $\frac{1}{6}\pi$ as those of the P, D and G surfaces with corresponding symmetry. The Poincaré representation of this hyperbolic plane (Coxeter 1961) is shown in figure 11. All points of the plane fall inside a circle, points at infinity are on the circle and geodesics appear as

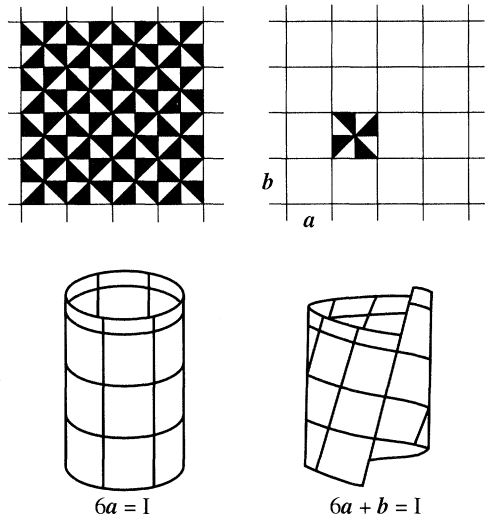

Figure 12. Construction of two different cylindrical surfaces by identifications in the flat plane tiled with an orthoscheme triangle having vertex angles of $\frac{1}{2}\pi$, $\frac{1}{4}\pi$ and $\frac{1}{4}\pi$.

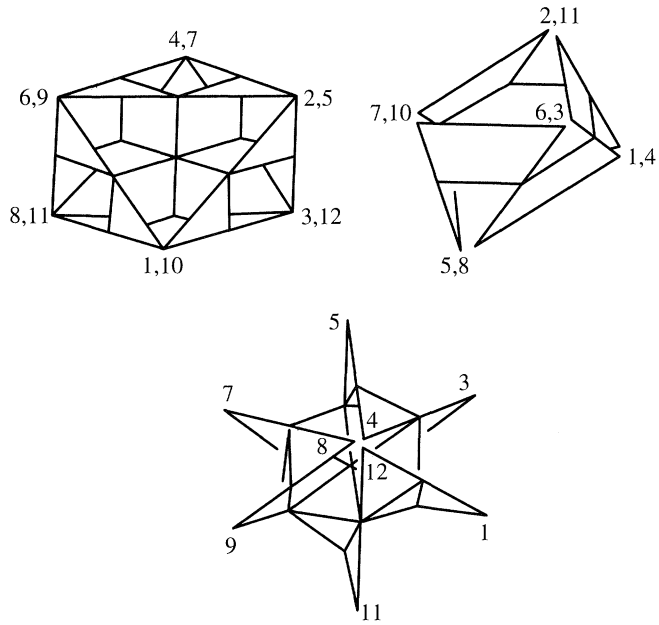

Figure 13. Topological equivalents showing the identifications of the vertices of the dodecagonal cell of the hyperbolic plane leading to the cells of the P, D and G surfaces.

circular arcs meeting the limiting circle normally. Since the representation is conformal, angles are preserved, particularly those of the orthoscheme triangles which are easily recognizable on the figure. Using such a mapping the length of a constant segment changes as it is displaced from the centre to the periphery. The figure shows that the representation can be tiled with hexagons which meet four at every vertex; this is the tiling $\{6, 4\}$ already discussed, impossible on a flat plane, where hexagons meet three at each vertex, but which is possible on a saddle surface.

(*f*) *Symmetry groups and dodecagonal cell*

The orthoscheme triangle is the fundamental region of the symmetry group of the hyperbolic pattern. It is repeated by reflections about its edges to cover the whole surface without overlap. Among all possible products of reflections, some correspond to translations on the surface and constitute a translation subgroup. If we limit ourselves to translations which can be identified with the building of a torus of topological genus 3, the fundamental region of the hyperbolic plane for this subgroup of translations is the dodecagon shown in figure 11. This dodecagon is a set of 96 orthoscheme triangles, arranged in exactly the same manner as those in the dodecagonal piece of surface contained in the cells of each of the three TPMS. The possible writing of certain translations as identities corresponds to the three groupings of vertices observed on the TPMS. We do not detail this here, but use a simple analogy to convey the idea contained in Sadoc & Charvolin (1989), see also Firby & Gardiner (1982). This analogue is the flat plane in our Euclidean three-dimensional space, built with an orthoscheme triangle having vertex angles of $\frac{1}{2}\pi$, $\frac{1}{4}\pi$ and $\frac{1}{4}\pi$. In this case the elementary cell of the simplest translation subgroup is a square of eight orthoscheme triangles and the choice of certain identifications, materialized by cutting of the plane and deforming a piece of this plane by bending without stretching to write certain translations as identities, permits the building of different cylindrical surfaces with the same zero Gaussian curvature as the initial plane, as shown in figure 12. The same operations on the hyperbolic plane, keeping its Gaussian curvature constant in its embedding space, permit the building of topological equivalents of the cells of the three TPMS in this space. Three-dimensional models of these equivalents, and of the cells, are shown in figure 13. We insist that we have not yet obtained the TPMS, but just topologically equivalent surfaces with uniform Gaussian curvature, embedded in the space of the hyperbolic plane. The next step would consist in embedding these topological equivalents in our space, but this would require a redistribution of the Gaussian curvature, at constant mean value. The lengths of the edges of the orthoscheme triangle, but not their angles, would be changed during this process.

(*g*) *Other approaches*

We have analysed the relationship between these three TPMS topologically, but other points of view are possible; for instance, an analytical approach, expressed in the Bonnet transformation (Schoen 1970; Hyde & Andersson 1984), or crystallographically, based on the methods recently developed for quasi-crystals (Mosseri & Sadoc 1990).

The coordinates of the D, P, and G surfaces can be expressed as functions of an angular parameter θ (the Bonnet angle) in the Weierstrass representation. As this parameter is varied continuously from 90° to 0°, a set of surfaces is obtained. The surfaces F, G, and P appear for 90°, 38.015° and 0°, respectively, and are the only surfaces without self-intersection. This Bonnet transformation, of one surface into another, proceeds at constant Gaussian curvature.

The quadrilateral patch of surface G shown in figure 5 was calculated from those of surfaces D and P shown in figures 3 and 4 using the analytical expression for this transformation.

The same three surfaces can be obtained as three-dimensional bounded projections along three different directions of one unique surface built in a space of six dimensions. The example of two-dimensional cuts through a three-dimensional sim-

PHILOSOPHICAL TRANSACTIONS OF THE ROYAL SOCIETY A MATHEMATICAL, PHYSICAL & ENGINEERING SCIENCES

ple cubic lattice may convey the idea. The two-dimensional lattice of a [100] cut is quadratic whereas that of a [111] cut is triangular. The G surface appears as a three-dimensional bounded projection in an oblique space relative to the two spaces leading to the P and D surfaces (Mosseri & Sadoc 1990).

(*h*) *Physical transformations*

The transformations discussed above imply either cuts or self-intersections which have no physical significance. Structural studies in phase diagrams showing coexisting cubic phases suggest indeed that one structure transforms into another by a deformation of its cell and slipping of the branchings of the rods of the labyrinths (Barois *et al.* 1990; Rawiso & Charvolin 1989, unpublished results). Why one structure is more stable than another is not clearly understood, but the area-to-volume ratio may be the important factor (Barois *et al.* 1990).

5. Prolamellar bodies (PLB) in etioplasts

Observations of plant meristem cells by electron microscopy show that the internal membranes of their plastids build remarkably ordered bicontinuous structures. The grana and frets of the chloroplasts appear when the plant grows in the light, and the prolamellar bodies of the etioplasts when the plant grows in the dark (Gunning & Steer 1975). The topologies and symmetries of these structures are independent of the species of the plant studied and, in some cases, these structures may be partly controlled by the ionic strength of the surrounding medium. They may even be reconstituted after having been isolated *in vitro* (Gunning & Steer 1975 and references therein). We describe here only the prolamellar bodies of etioplasts, the basic organization of which is astonishingly close to that of the liquid crystalline cubic phases.

(*a*) *Structures*

Prolamellar bodies (PLB) which are thought to be membraneous storage organizations, can be described as ordered networks of branched tubular units with bicontinuous topology. Analysis of micrographs of serial sections of PLB obtained by electron microscopy suggest two models of branched tubular units: one with six orthogonal arms (Granick 1961), as in the $Im\bar{3}m$ structure or P surface, the other with four arms at angles of 109°28′ (Wehrmeyer 1965), as in the $Pn\bar{3}m$ structure or the D surface. It seems now that six-armed units are rather rare, if they exist at all (Gunning & Steer 1975; Murakami *et al.* 1985), and we consider only tetrahedral units.

The four-armed unit is shown in figure 14, the membrane thickness being about 60 Å, as in liquid crystals, and the tubules have an external diameter of about 350–380 Å, larger than that in liquid crystals by a factor of about six. These units can be assembled in four main ways which are described in Gunning & Steer (1975): a diamond or zinc blende-type network, identical to that of the D surface, a wurtzite-type hexagonal network, and the open lattice and centric organizations.

(*b*) *Open lattice PLB*

The openlattice PLB can be described as a periodic assembly with space group $Fd3m$ of two slightly distorted polyhedra, regular dodecahedra with pentagonal faces and irregular hexakaidecahedra with pentagonal and hexagonal faces, as shown in

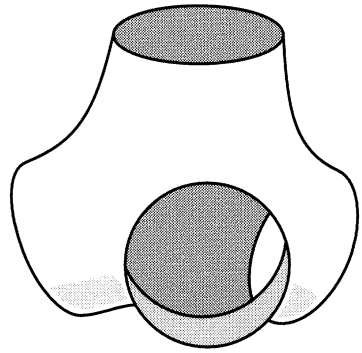

Figure 14. The four-armed branched tubular unit of prolamellar bodies, the thickness of the membrane and the external diameter of the tubular arms are of about 60 and 350–380 Å, respectively.

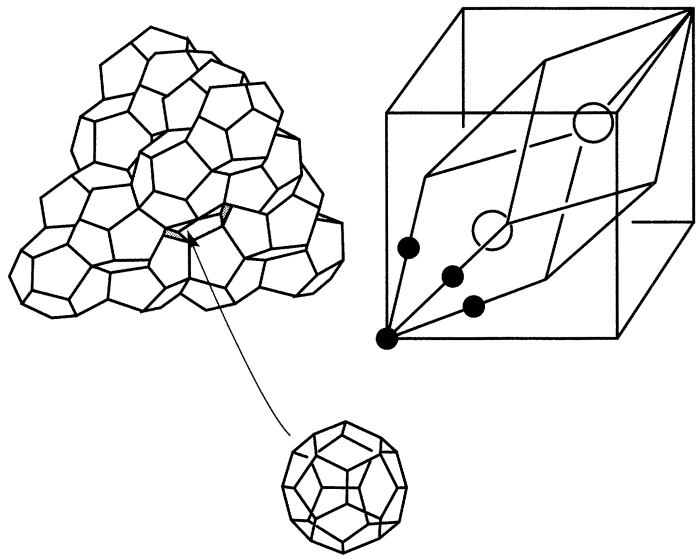

Figure 15. Tetrahedral aggregation of slightly distorted dodecahedra with one hexakaidecahedron in the center, on the right the positions of the dodecahedra (•) and hexakaidecahedra (○) in the elementary crystallographic cell of volume $\frac{1}{4}$ of that of the $\{Fd3m\}$ cell (Williams 1979).

figure 15, the axes of the tubules being aligned along the edges of the polyhedra. The edge of the cubic unit cell is about 2800 Å.

(*c*) *Centric PLB*

In figure 16, at the centre, the four-armed tubular units build a pentagonal dodecahedron; on the twelve faces of this dodecahedron the units are organized along twelve pentagonal columns radiating outwards. Each set of three columns surrounding a vertex of the dodecahedron can be seen as the edges of a tetrahedral space within which the units are arranged according to the same symmetry as that of the zinc blende, i.e. with their axes aligned along the rods of one labyrinth of the D surface. The connections between units of two adjacent tetrahedra then require the interfacial regions to follow the wurtzite form of zinc sulphide. The overall shape of the assembly is icosahedral with five-fold symmetry axes along the pentagonal columns and the overall diameter of a centric PLB is in the range 10^3–10^4 Å.

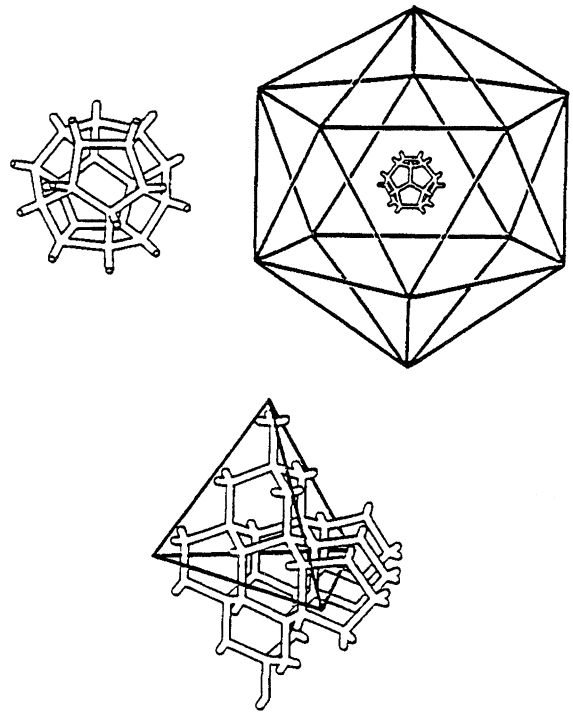

Figure 16. Elements for the description of a centric prolamellar body: the central pentagonal dodecahedron with 20 vertices and 12 faces, the overall icosahedron with 12 vertices (corresponding each to a face of the central dodecahedron) and 20 faces (corresponding each to a vertex of the central dodecahedron), one of the tetrahedra, determined by each face of the icosahedron and its centre, with the zinc blende (inside), wurtzite (face) and pentagonal column (edge) organizations of the units (the diameter of the tubules is not to scale for readability).

(*d*) *Deviations from the surfaces described previously*

These structures are obviously bicontinuous like those described previously, but differ from them, not only by the appearance of five-fold symmetries, but also by the fact that the two subspaces separated by the surface of the membrane are not congruent. For instance, in the tetrahedral domains of the centric PLB, where the labyrinths are those separated by the D surface, the mid-surface of the membrane is at a distance from this exact D surface (Murakami *et al.* 1985). We propose that these structures (with five-fold symmetries) are distorted to cancel the cost in curvature energy introduced by no longer being minimal.

6. Arguments for the formation of such structures in PLB

The physical arguments applied to liquid crystalline structures are not valid in this case. First, the characteristic dimensions of the structures are larger by about a factor of six, so that the constraint put on the distance between interfaces of films of similar thickness is weaker, and second, lipids with a high water content tend to keep their interfaces flat, so that there is no constraint of interfacial curvature. An approach to these etioplast structures might be found in the observations of the formation of passages connecting adjacent films in multilamellar vesicles which are ordered into a bicontinuous structure of the $Pn\bar{3}m$ type with characteristic distances

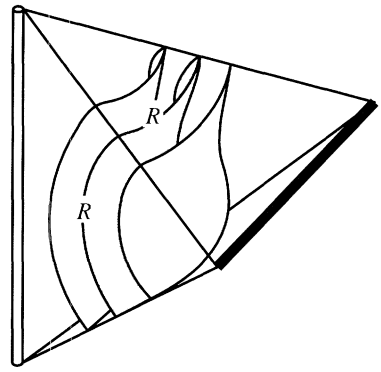

Figure 17. A patch of minimal surface (hatched) separating segments of two labyrinths; the moduli of its principal curvature radii are equal, those of a parallel surface at a distance d are $R + d$ so that its mean curvature goes as $2d/(R^2(1 - (d/R)^2))$ and its Gaussian curvature as $-1/(R^2(1 - (d/R)^2))$.

even larger than those of PLB (Harbich *et al.* 1978). It is proposed in this case that two parallel films coming into contact, because of thermal fluctuations, fuse and build a passage of low mean curvature and negative Gaussian curvature, which is eventually stabilized because of a positive Gaussian curvature constant (Harbich *et al.* 1978). Several passages could gather together because an attractive interaction between two passages on either sides of one film would minimize the energy of mean curvature (Fourcade, personal communication).

In the case of PLB, a theory must include the fact that they develop by the growth of the membrane, including new lipids in it (Gunning & Steer 1975), and, as one of the subspaces is connected to the outside and the other not, this unbalanced growth must affect the organization. For example, starting from the structure of the D surface, as the area-to-volume ratio increases on one side of the surface, the surface can no longer be minimal and we propose that the formation of pentagonal rings of tubules among the hexagons is a way of decreasing the cost in curvature energy (Charvolin 1994).

We start from a membrane forming a D surface in a $Pn\bar{3}m$ structure. This separates two subspaces with equal volumes, the skeletons of which are networks of the zinc blende-type with hexagonal rings. We assume that the membrane has no spontaneous curvature. The two volumes separated by the membrane become unequal, as is observed in PLB, if its middle surface is no longer on the TPMS but on a surface parallel to it at a given distance d, and the space group of the structure changes to $F\bar{4}3m$. In this case the membrane must have a non-zero mean curvature of value d/R^2, as shown in figure 17, and this implies an energy cost which can be written as

$$E_c = \tfrac{1}{2}\kappa(C_1 + C_2)^2.$$

This value of the mean curvature can be related to the parameter a of the cell using classical formulae for the TPMS (Hyde 1990; Hyde & Andersson 1984):

$$\langle 1/R^2 \rangle = -8\pi/A_0, \quad A_0 = 2.4V_0^{2/3}, \quad V_0 = a^3,$$

where V_0 and A_0 are the volume of the cell and the area of TPMS contained in it, respectively. From the observations in Murakami *et al.* (1985),

$$a \simeq 2 \times 390 \text{ Å}, \quad d = 20 \text{ Å},$$

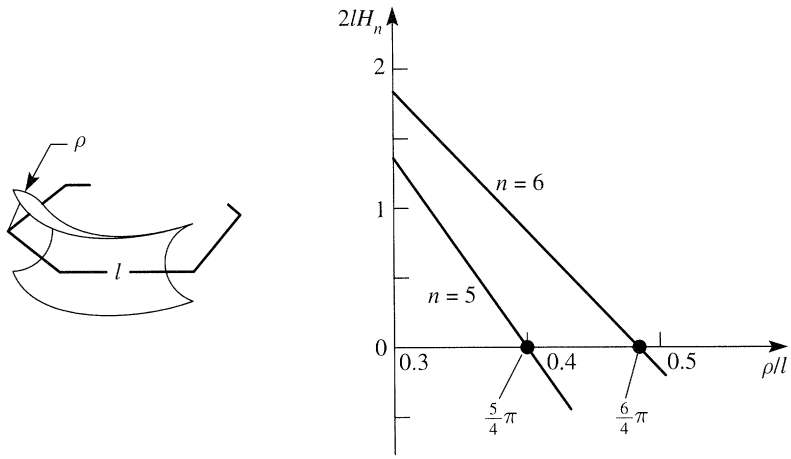

Figure 18. A portion of a ring of n sides of length ℓ with its associated toroidal patch of membrane surface of smallest radius ρ and the evolution of the estimated mean curvature H_n of the surface with for two values of n.

and the mean curvature on the parallel surface is

$$H_{\mathrm{d}} \simeq 3.4 \times 10^{-4}\ \text{Å}^{-1}.$$

This mean curvature, and hence its associated energy cost, could be decreased, or even suppressed, if the $F\bar{4}3m$ structure with a tetracoordinated network of hexagonal rings transforms into a structure with a tetracoordinated network but with pentagonal rings with smaller angles between the sides of the rings (108° instead of 109°28′). This can be readily seen using a simple model of hexagonal and pentagonal rings having the same side length l and tubules with the same radius ρ (these two points are supported by the coexistence of the two types of rings in a centric PLB), and calculating local mean curvatures on the toroidal surface at the inside of the ring where the curvature is concentrated, as shown in figure 18. The local mean curvature on the inside part of a ring with n sides can be written as

$$2\ell H_n = (\rho/\ell)^{-1} - (n/2\pi - \rho/\ell)^{-1},$$

and the corresponding curves show that if ρ decreases from the value $6\ell/4\pi$, the radius of the tubules of the TPMS with zero mean curvature and hexagonal rings, the mean curvature increases but can be decreased if hexagonal rings become pentagonal, and even be suppressed when ρ attains the value $5\ell/4\pi$. From the observation in Murakami *et al.* (1985),

$$\rho = 140\ \text{Å}, \quad \ell = 337\ \text{Å},$$

and the decrease in mean curvature is

$$H_6 - H_5 \simeq 10^{-3}\ \text{Å}^{-1}.$$

The decrease $H_6 - H_5$ has the same order of magnitude as H_{d} so that the curvature energy cost which would appear if the middle surface of the membrane stayed parallel to a D surface with hexagonal rings can indeed be cancelled by its transformation into a structure with pentagonal rings. (A minimal surface with catenoid ends, very similar to the dodecahedral core of the centric PLB, was recently calculated by Berglund & Rossman, personal communication.)

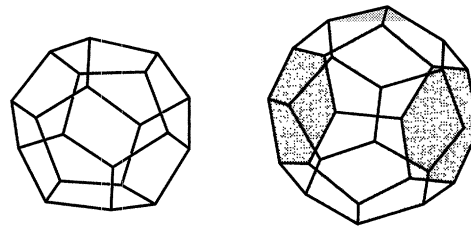

Figure 19. Transformation of a dodecahedron into a hexakaidecahedron by four half disclination lines of value $-\frac{2}{5}\pi$ each; hexagons created from pentagons are hatched.

(*a*) *A common structural basis, another example of frustration and its relaxation in* S^3

A regular tetra-coordinated network of pentagonal rings only would be that formed by the edges of an assembly of regular dodecahedra packed three around each edge and four around each vertex. As is well known, it is impossible to build such an assembly in our flat three-dimensional space R^3, as the dihedral and edge angles of the dodecahedron are smaller than 120° and 109°28′ or, in other words, the local organization with five-sided rings imposed by the curvature of the membrane cannot propagate in our space. This is another expression for a frustration, a conflict between short- and long-range topological orders. Fortunately, as in the liquid crystalline case, it is possible to relax this frustration in the curved space S^3 where an assembly of regular dodecahedra is possible and known as the $\{5,3,3\}$ polytope (Coxeter 1961); this polytope can be seen as an ideal template for a structure with pentagonal rings only. The existence of minimal surfaces in S^3 which do not separate S^3 in two identical subspaces was shown by Karcher *et al.* (1988), but the case of a surface built around the edges of $\{5,3,3\}$ was not considered. The structures possible in R^3 are obtained from $\{5,3,3\}$ by mapping or projection of the curved space S^3 onto the flat space R^3.

(*b*) *The crystalline structure of open lattice PLB*

Starting from $\{5,3,3\}$ in S^3, the introduction of disclinations realizes its mapping onto R^3. These disclinations cannot be along the edges of the polyhedra, as the only possible ordered structure obtained that way would be another polytope $\{5,3,4\}$, which does not exist in R^3 but in a hyperbolic space with negative Gaussian curvature, they must be perpendicular to the faces of the polyhedra. Such disclinations transform the regular dodecahedron into an irregular tetrakaidecahedron, pentakaidecahedron or hexakaidecahedron (14, 15 or 16 faces), as shown in figure 19, and these polyhedra can be packed with dodecahedra to build ordered space-filling assemblies of cells at the expense of slight distortions (Williams 1979). Among the structures built in this way is one which has space group $Fd\bar{3}m$ and a crystallographic unit cell which contains 16 dodecahedra and eight hexakaidecahedra. This is the structure of the open lattice PLB, shown in figure 15. This complex structure is indeed well known in other domains of condensed matter physics. For instance, a non-bicontinuous liquid crystalline structure; the cubic micellar structure, where a film of amphiphiles supported by the faces of the polyhedra defines closed cells entrapping droplets of water; type-II clathrates of water molecules, where their bonds aligned along the edges of the polyhedra build cages entrapping host molecules; and Laves phases of metallic alloys. The relationship between these systems of very different physico-chemical natures is due to the fact that the space-filling problem in the cases

of tetracoordinated atoms or molecules, the propagation of a local tetrahedral order, is also impossible in R^3 and that the template which reconciles tetracoordination and compaction is the polytope $\{3,3,5\}$ of S^3, which is the dual of $\{5,3,3\}$ (Sadoc & Charvolin 1992).

(c) *The icosahedral cluster of centric PLB*

Such a cluster was first proposed to account for the short-range order in tetracoordinated amorphous semiconductors, such as germanium or silicon. The arrangements of the atoms and the bonds between them are exactly the same as those of the branched units and their tubules in a centric PLB (Gaskell 1975; Mosseri & Sadoc 1985). As before the two problems are the dual of each other and the mapping of S^3 onto R^3 introduces distortions which manifest themselves through the appearance of hexagonal rings among the pentagons of the $\{5,3,3\}$ polytope. In this approach, the regions similar to the template, with pentagonal rings, are the topologically ordered regions and those where the configuration differs from that of the template, with hexagonal rings, are the defects. This is a convention opposite to that followed by previous authors in describing centric PLB (Gunning & Steer 1975; Murakami *et al.* 1985).

7. Comments

We have described six ordered bicontinuous structures, three being formed by films of amphiphiles in liquid crystals and three by membranes in biological systems, and we have proposed to integrate them within the same topological and structural frame by making reference to minimal surfaces and more particularly triply periodic minimal surfaces. For the three liquid crystalline structures ($Pn\bar{3}m$, $Im\bar{3}m$ and $Ia\bar{3}d$) we have enough physics and mathematics to relate observed structures and calculated TPMS (F and P surfaces of Schwarz, G surface of Schoen). For the three biological structures (zinc blende, open lattice and centric PLB) the ground is less firm. They are well described, but the parameters controlling them have not yet been established and, except for the first (which can be related to the D surface), the other two have no obvious relation to known minimal surfaces.

However, strong structural correspondences can be established between these two structures of the living world and those of inert materials (water clathrates, Laves phases of metals and alloys, amorphous semiconductors) which are compromises between two incompatible requirements. The local topological order imposed by the atoms or molecules is not compatible with the Euclidean structure of our space. Similarly for the open lattice and the centric PLB. we proposed that they can be looked at as distortions of the zinc blende PLB in response to the pushing off balance of its supporting D surface during the growth process of the membrane.

Finally, more can be said about the icosahedral cluster of the centric PLB. Five-fold symmetry and icosahedral organizations are most common in living systems, either at the microscopic level of the icosahedral capsids of viruses or at the macroscopic level of organisms such as radiolaria, sea-stars and flowers. The rule for the building of the capsids lies in the symmetry of the basic aggregates of proteins constituting them and that for their selection is that the icosahedral surface is nearly spherical, i.e. the number of proteins involved is the smallest for a given volume. There is not such a clear argument for the macroscopic examples. We think that the system considered here might help to introduce a new point of view. First, its typical size

PHILOSOPHICAL TRANSACTIONS OF THE ROYAL SOCIETY A MATHEMATICAL, PHYSICAL & ENGINEERING SCIENCES

is intermediate between those of the viruses and the organisms quoted above, and second, its behaviour suggests an argument for the occurrence of five-fold symmetry on a large scale even though its molecules, the lipids, and their aggregation state, at the interfaces of the membrane, do not contain any symmetry element of this order. As we have demonstrated, the necessity for the membrane to minimize its curvature energy under the action of a uniform constraint applied over its whole surface might force it to adopt a configuration where five-fold symmetry is dominant. This would be a remarkable example of how a local property, the curvature of the membrane, determines a global property, the five-fold symmetry, in a living material.

References

Barois, P., Eidam, D. & Hyde, S. T. 1990 *J. Physique* **51**, C7-25–34.

Charvolin, J. 1995 In *Interplay of genetic and physical process in the development of biological forms* (Les Houches Winter School 1994) (ed. F. Gaill & D. Beyssens). Singapore: World Scientific.

Charvolin, J. & Sadoc, J.-F. 1987 *J. Physique* **48**, 1559–1569.

Charvolin, J. & Sadoc, J.-F. 1994 In *Micelles, membranes, microemulsions and monolayers* (ed. W. M. Gelbart, A. Ben-Shaul & D. Roux). Berlin: Springer.

Coxeter, H. S. M. 1961 *Introduction to geometry.* New York: Wiley.

Dubois-Violette, E. & Pansu, B. (eds) 1990 International workshop on geometry and interfaces. *J. Physique* **51**, C7.

Firby, P. A. & Gardiner, C. F. 1982 *Surface topology.* New York: Ellis Horwood.

Friedel, J. 1984 In *Proc. 6th General Conf. of the EPS* (Prague).

Gaskell, P. M. 1975 *Phil. Mag.* **32**, 211.

Gelbart, W. M., Ben-Shaul, A. & Roux, D. (eds) 1994 *Micelles, membranes, microemulsions and monolayers.* Berlin: Springer.

Gunning B. E. S. & Steer, M. W. 1975 *Ultrastructure and the biology of plant cells.* London: Arnold.

Granick, S. 1961 In *The cell, biochemistry, physiology, morphology* (ed. S. Brachet & A. E. Mirsky), vol. II, p. 489. New York: Academic.

Harbich, W., Servuss, R. M. & Helfrich, W. 1978 *Z. Naturf.* a **33**, 1013.

Helfrich, W. 1990 In *Liquids at interfaces* (Les Houches Summer School Session XLVIII) (ed. J. Charvolin, J.-F. Joanny & J. Zinn-Justin). Amsterdam: North-Holland.

Hilbert, D. & Cohn-Vossen, S. 1983 *Geometry and the imagination.* New York: Chelsea.

Hyde, S. T. 1990 *J. Physique* **51**, C7-209.

Hyde, S. T. & Andersson, S. 1984 *Z. Kristallogr.* **168**, 221–254.

Karcher, H., Pinkall, U. & Sterling, I. 1988 *J. Diff. Geom.* **28**, 169.

Lindblom, G. & Rilfors, L. 1989 *Biochim. Biophys. Acta* **988**, 221.

Lipowsky, R. (ed.) 1992 *The structure and conformation of amphiphilic membranes* (Springer Proceedings in Physics 66).

Luzzati, V. & Spegt, P. A. 1967 *Nature* **215**, 701.

Mackay, A. L. 1985 *Nature* **314**, 604–606.

Mariani, P., Luzzati, V. & Delacroix, H. 1988 *J. Mol. Biol.* **204**, 165.

Mosseri, R. & Sadoc, J.-F. 1985 *J. Non-crystall. Solids* **77**, 179.

Mosseri, R. & Sadoc, J.-F. 1990 *J. Physique* **51**, C7-257.

Murakami, S., Yamada, N., Nagano, M. & Osum, M. 1985 *Protoplasma* **128**, 147.

Nelson, D., Piran, T. & Weinberg, S. (eds) 1989 *Statistical mechanics of membranes and surfaces.* Singapore: World Scientific.

Sadoc, J.-F. & Charvolin, J. 1989 *Acta Crystallogr.* A **45**, 10–20.

PHILOSOPHICAL TRANSACTIONS OF THE ROYAL SOCIETY A MATHEMATICAL, PHYSICAL & ENGINEERING SCIENCES

Sadoc, J.-F. & Charvolin, J. 1992 *J. Physique* I **2**, 845–859.

Schoen, A. H. 1970 NASA Technical Note, D-5541.

Schöenflies, A. 1882 *C. R. Acad. Sci., Paris* **112**, 478.

Schwarz, H. A. 1890 *Gesammelte Mathematische Abhandlungen.* Berlin: Springer.

Seddon, J. M. 1989 *Biochim. Biophys. Acta* **1031**, 1.

Thomas, E. L., Alward, D. B., Kunning, D. J., Martin, D. C., Handlin, D. J. & Fetters, L. J. 1986 *Macromolecules* **20**, 1651.

Wehrmeyer, W. Z. 1965 *Z. Naturf.* b **20** 1270, 1278, 1288.

Williams, R. 1979 *The geometrical foundation of natural structures.* New York: Dover.

PHILOSOPHICAL TRANSACTIONS OF THE ROYAL SOCIETY A MATHEMATICAL, PHYSICAL & ENGINEERING SCIENCES